HHS Public Access

Author manuscript

Neuron. Author manuscript; available in PMC 2016 December 02.

Published in final edited form as:

Neuron. 2015 December 2; 88(5): 918–925. doi:10.1016/j.neuron.2015.10.042.

Presynaptic deletion of GIT proteins results in increased synaptic strength at a mammalian central synapse

Mónica S. Montesinos[1], **Wei Dong**[1], **Kevin Goff**[1], **Brati Das**[1,2], **Debbie Guerrero-Given**[3], **Robert Schmalzigaug**[4], **Richard T. Premont**[4], **Rachel Satterfield**[1], **Naomi Kamasawa**[3], and **Samuel M. Young Jr**[1,*]

[1]Research Group Molecular Mechanisms of Synaptic Function, Max Planck Florida Institute for Neuroscience, Jupiter, FL 33458 USA

[2]Integrative Program in Biology and Neuroscience, Florida Atlantic University, Jupiter, FL 33458 USA

[3]Max Planck Florida Institute for Neuroscience Electron Microscopy Facility, Jupiter FL 33458 USA

[4]Divison of Gastroenterology, Department of Medicine, Duke University Medical Center, Durham, NC, 27710 USA

Abstract

A cytomatrix of proteins at the presynaptic active zone (CAZ) controls the strength and speed of neurotransmitter release at synapses in response to action potentials. However, the functional role of many CAZ proteins and their respective isoforms remains unresolved. Here, we demonstrate that presynaptic deletion of the two G-protein-coupled receptor kinase-interacting proteins (GITs), GIT1 and GIT2, at the mouse calyx of Held leads to a large increase in AP-evoked release with no change in the readily releasable pool size. Selective presynaptic GIT1 ablation identified a GIT1 specific role in regulating release probability that was largely responsible for increased synaptic strength. Increased synaptic strength was not due to changes in voltage gated calcium channel currents or activation kinetics. Quantitative electron microscopy revealed unaltered ultrastructural parameters. Thus, our data uncover distinct roles for GIT1 and GIT2 in regulating neurotransmitter release strength, with GIT1 as a specific regulator of presynaptic release probability.

*Correspondence: Samuel M. Young, Jr. PhD, Max Planck Research Group Leader, Research Group Molecular Mechanisms of Synaptic Function, Max Planck Florida Institute for Neuroscience, One Max Planck Way, Jupiter, Florida 33458 USA, sam.young@mpfi.org, Office: +1 561-972-9402, Fax: +1 561-972-9001.

SUPPLEMENTAL INFORMATION

Supplemental Experimental Procedures, four figures and two tables and can be found with this article online.

Author Contributions

M.S.M., W.D., K.G., B.D., D.G.G., N.K., and S.M.Y., Jr. designed experiments, carried out experiments and analyzed data. R.S. produced rAd vectors. M.S.M. and S.M.Y., Jr. wrote the manuscript. R.S and R.T.P provided mouse lines and edited the manuscript.

Introduction

The release probability (P_r) of synaptic vesicles (SVs) in response to action potentials (APs), from a pool of fusion competent SVs, the readily releasable pool (RRP), regulates synapse strength (Regehr, 2012). Critical to the regulation of SV release at the active zone (AZ) is an electron dense network of proteins, the cytomatrix at the active zone (CAZ) which regulate SV release through distinct pathways (Gundelfinger and Fejtova, 2012). A family of functionally conserved molecules, the G-protein-coupled receptor (GPCR) kinase-interacting proteins (GITs) are located in the CAZ and function as part of an oligomeric complex with PIX proteins, which serve as a scaffold for numerous signaling partners (Hoefen and Berk, 2006).

In mammals, two genes, *Git1* and *Git2*, encode GITs which share highly conserved domain structures and amino acid sequences (Hoefen and Berk, 2006). In the CNS, GITs are widely co-expressed (Schmalzigaug et al., 2007) and localized within both, pre- and postsynaptic compartments (Ko et al., 2003). In *D. melanogaster* and *C. elegans*, a single conserved GIT ortholog is ubiquitously expressed (Bahri et al., 2009; Lucanic and Cheng, 2008). *Git2* knockout (KO) mice are viable but have hearing impairments (White et al., 2013) and anxiety-like behaviors (Schmalzigaug et al., 2009b). Unlike *Git2* KO mice, most *Git1* KO mice die at birth, and adult survivors have impaired fear memory (Schmalzigaug et al., 2009a), operant conditioning (Menon et al., 2010) and spatial and object learning (Won et al., 2011). In addition, GIT1 has been implicated in Huntington's disease (Goehler et al., 2004) and attention deficit hyperactivity disorder (Won et al., 2011) although this is controversial (Klein et al., 2015).

Although GIT1 function has been characterized in the postsynaptic compartment (Segura et al., 2007; Zhang et al., 2003), due to the inability to selectively ablate presynaptic GIT expression, little is known about GIT function at the mammalian presynapse. The calyx of Held/medial nucleus of the trapezoid body (MNTB) is a giant glutamatergic axosomatic synapse in the auditory brainstem, which tightly regulates RRP release dynamics to support the early stages of auditory processing (Borst and Soria van Hoeve, 2012). Due to its unparalleled experimental accessibility, presynaptic mechanisms of synaptic transmission can be analyzed independent of postsynaptic contributions. Thus, this is an ideal synapse to address presynaptic GIT functions in synaptic transmission regulation. Here, we used *Git1* conditional knockout (CKO) (*Git1*$^{-/-}$, in presence of Cre recombinase), *Git2* KO (*Git2*$^{-/-}$) and *Git1* CKO/*Git2*KO (*Git1*$^{-/-}$/*Git2*$^{-/-}$) transgenic mice, together with our ability to conditionally ablate GIT1 expression in the calyx of Held, to analyze role GITs in synaptic transmission. We show that loss of both GIT1 and GIT2 results in increased AP-evoked release but with no change in RRP size, SV number or distribution at the AZ, voltage gated calcium channels currents or calyx morphology. However, individual ablation of *Git1* increased P_r, while ablation of *Git2* did not. Our data demonstrate that GIT1 and GIT2 proteins regulate synaptic strength through distinct presynaptic mechanisms that increase exocytosis efficiency, with distinct role for GIT1 regulation of P_r.

Results

GIT protein expression at the calyx of Held

Since the GITs expression pattern at the calyx of Held was unknown, we carried out immunohistochemical (IHC) staining on the P18-21 calyx of Held. Our results indicated that GIT1 and GIT2 could be detected in the calyx. Line scan analysis indicated that GIT1 and GIT2 colocalized with vesicular glutamate transporter 1 (VGLUT1) (Figure S1A, B). Our results confirm prior studies where GIT1 was found at hippocampal presynapse (Ko et al., 2003; Podufall et al., 2014) and demonstrate GIT2 is also expressed presynaptically.

GIT1 and GIT2 regulate AP-evoked release

In order to selectively ablate GIT1 expression or ablate all GIT expression at the calyx, we injected a rAd that independently co-expressed Cre and EGFP, using a stereotactic injection approach into the cochlear nucleus (CN) of P0-1 *Git1* CKO or *Git1*CKO/*Git2* KO mice (See Supplemental Experimental Procedures). This permitted specific analysis of GIT1 presynaptic function independent of its postsynaptic role which was not possible in previous studies using *Git1* KO animals (Menon et al., 2010; Schmalzigaug et al., 2009a). In addition, ablating GIT1 presynaptically and GIT2 expression globally, we were able to examine how complete loss of GITs affected presynaptic function.

To analyze how the individual and combined GIT proteins regulated AP-evoked release, we performed midline stimulation of calyx axons while the resultant AMPA excitatory postsynaptic currents (EPSCs) from principal cells of the MNTB innervated by transduced and non-transduced P18-21 calyces were recorded in whole-cell voltage clamp mode (See Supplemental Experimental Procedures). To determine how GITs affect basal synaptic transmission, we used a stimulation frequency of 0.05 Hz. Loss of both GIT1 and GIT2 together led to a 2-fold increase in the AP-evoked EPSCs compared to wild type (WT) (9.01 ± 1.44 nA, n=18 vs. 4.52 ± 0.75 nA, n=13; $p<0.05$). Loss of GIT2 had no effect, while loss of GIT1 showed a trend towards increased AP-evoked release, but did not reach statistical significance (Figure 1A–C, table S1). Expression of Cre alone had no effect on AP-evoked release (Figure S2A–D, table S1). Analysis of normalized AP-evoked EPSC waveforms revealed that GIT loss did not affect AP-evoked release kinetics (Figure 1D). Analysis of mEPSC revealed no changes in mEPSC frequency or kinetics (Figure S3, table S1). These results demonstrate that GITs regulate synaptic strength at mammalian CNS synapses.

Loss of GIT1, but not GIT2, increases initial release probability

Increased AP-evoked release could be explained in two ways: 1) an increase in RRP size or 2) an increase in initial P_r. To determine the RRP size, we carried out afferent fiber stimulation at 100 Hz, plotted the data using the back extrapolation method (Schneggenburger et al., 1999) and by using the methodology of Elmqvist and Quastel (EQ) (Figure S4) (Elmqvist and Quastel, 1965). Subsequent analysis revealed that individual loss of GIT1 or GIT2 alone, or the combined loss of GIT1 and GIT2, did not lead to any statistically significant increase in the RRP size compared to WT (Figure1E–H, Figure S4 A–C), table S1). Expression of Cre alone had no effect on RRP size (Figure S2E–H, table

S2). Therefore, our functional measure of RRP size in the absence of GITs indicates RRP size changes are not responsible for increased AP-evoked release.

Since the RRP size was unchanged, the increased AP-evoked release was likely to be caused by increased P_r. To calculate the initial P_r, we divided the first EPSC amplitude from each train by the RRP size as calculated by the two different methods. Our results demonstrated that loss of GIT1 and GIT2 together led to a significant increase in initial P_r compared to WT (0.37 ± 0.02, n=18 vs. 0.26 ± 0.02, n=13; p<0.001) (Figure 1I, J). The same results are obtained by the EQ method (0.34 ± 0.02, n=18 vs. 0.18 ± 0.03, n=12; p<0.001) (Figure S4 D, E). Interestingly, GIT1 loss alone also led to similar increases in initial P_r compared to WT regardless of the method used (0.35 ± 0.02, n=10 vs. 0.26 ± 0.02, n=13; p<0.01) while GIT2 did not (Figure 1I, J). EQ method (0.34 ± 0.02, n=18 vs. 0.18 ± 0.03, n=12; p<0.001) (Figure S4 D, E). Expression of Cre alone did not change P_r compared to WT (Figure S2I, J, table S1).

To further confirm GIT1 regulates initial P_r, we applied a paired pulse stimulation protocol and calculated the paired pulse ratio (PPR) at 10, 50 and 100 Hz (Regehr, 2012). Specifically, decreases in the PPR are hallmarks of increases in P_r due to presynaptic regulation. Figure 2 shows that at all frequencies tested there was a significant reduction in the PPR in both the *Git1*$^{-/-}$ or *Git1*$^{-/-}$/*Git2*$^{-/-}$ calyces, but not the *Git2*$^{-/-}$ (Figure 2A, B, table S1). Expression of Cre alone had no effect on PPRs (Figure S2K, L, table S1). These results show that deletion of GITs increased synaptic strength independent of increased RRP size. We conclude that GIT1 is the dominant isoform that regulates initial P_r at the calyx leading to changes in synaptic strength. In contrast, GIT2 contributes to synaptic strength increases independent of initial P_r regulation.

Loss of GIT1 and combined loss of GIT1 and GIT2 increases short-term depression

Since the initial P_r is increased without changes in the RRP size, this should lead to an increase in the rate of depression in response to a train stimulation. We analyzed the RRP release kinetics at 10, 50 and 100 Hz. We found an increase in the rate of onset of depression and lower steady state levels with the loss of GIT1 alone, and this amount of depression was not increased with loss of both GIT1 and GIT2 together (Figure 2C, D, table S1). Furthermore, unlike the WT or *Git2*$^{-/-}$ responses, *Git1*$^{-/-}$ and *Git1*$^{-/-}$/*Git2*$^{-/-}$ responses were best fit with a double exponential (Table S3). Expression of Cre resulted in no changes compared to WT (Figure S2M, N, table S1). Since loss of GIT1 alone led to an increase in frequency dependent depression, and with no further increases with the loss of GIT1 and GIT2 together, our data demonstrate that GIT1 regulation of P_r is the major determinant impacting frequency dependent synaptic plasticity.

Loss of GIT proteins does not affect voltage gated calcium currents

Changes in presynaptic calcium currents (I_{ca}) have dramatic effects on AP-evoked release (Regehr, 2012). To determine if increased I_{ca} might explain the initial P_r increase with loss of GIT1 or additional synaptic strength increase with loss of both GIT1 and GIT2,we measured the I_{ca} in the WT, *Git2*$^{-/-}$, *Git1*$^{-/-}$ and *Git1*$^{-/-}$/*Git2*$^{-/-}$ calyces. Analysis of the I_{ca} current-voltage (I/V) relationship demonstrated no change in the I_{ca} steady state amplitude

in the *Git1*$^{-/-}$ *or Git2*$^{-/-}$ calyces (Figure 3, table S1). However, there was a slight reduction in the *Git1*$^{-/-}$/*Git2*$^{-/-}$ calyces, but this did not reach significance. (Figure 3A–C, table S1). Normalization of I_{Ca} to the I_{Ca} maximum revealed no changes in the activation kinetics (Figure 3D). In addition, there was no change in I_{Ca} tail current peak amplitudes and activation kinetics (Figure 3E, F, table S1). Finally, C_{slow} values revealed no difference in calyx size between the WT and *Git1*$^{-/-}$, *Git2*$^{-/-}$ or *Git1*$^{-/-}$/*Git2*$^{-/-}$ calyces (Figure 3K).

Since our fiber stimulation experiments used APs to trigger SV release, we tested whether I_{Ca} influx triggered by a pseudo-AP waveform would be affected. To do so, we recorded the I_{Ca} evoked by pseudo-AP waveforms (Yang and Wang, 2006) (Figure 3G, H). Since the integral of I_{Ca} in response to an AP is the key determinant of the resultant EPSC, we measured the I_{Ca} charge in response to the pseudo-AP waveform and found no reduction in the I_{Ca} charge in *Git1*$^{-/-}$, *Git2*$^{-/-}$ or *Git1*$^{-/-}$/*Git2*$^{-/-}$ calyces compared to WT (Figure 3I). Since the loss of GITs did not affect I_{Ca} amplitude, charge or activation kinetics, this indicates that the loss of GITs proteins lead to an increased exocytosis efficiency, similar to what happens during calyx development (Taschenberger et al., 2002). Finally, we conclude that GIT1 regulation of P_r is independent of VGCC regulation.

Loss GIT proteins does not change SV distribution at the active zone

Since GITs interact with CAZ proteins implicated in AZ organization (Kim et al., 2003; Ko et al., 2003), it is possible that the increased exocytosis efficiency we observed in the *Git1*$^{-/-}$ and *Git1*$^{-/-}$/*Git2*$^{-/-}$ calyces was due to altered presynaptic substructure. To test this hypothesis, we acquired and analyzed electron microscopy (EM) images from WT, *Git2*$^{-/-}$, *Git1*$^{-/-}$ and *Git1*$^{-/-}$/*Git2*$^{-/-}$ calyces to assess if SV docking, SV distribution or AZ length were altered. Analysis of EM images revealed that SV distribution and number of docked SVs were not changed in any of the genotypes tested (Figure 4B–C, table S1) and there was only minor reduction in the AZ length in the *Git1*$^{-/-}$/*Git2*$^{-/-}$ compared to WT (262.1 ± 5.82 nm, n=120 vs. 293.6 ± 6.2 nm, n=125; $p<0.01$), (Figure 4D, table S1). Since docked SVs are correlated with RRP size (Schikorski and Stevens, 2001), these results are consistent with our previous observation that loss of GITs does not affect RRP size (Figure 1). In conclusion, our results indicate that loss of GITs does not affect synaptic substructure, SV docking or SV distribution relative to the AZ and are not the cause for increased P_r in the *Git1*$^{-/-}$ calyces or synaptic strength increases in the *Git1*$^{-/-}$/*Git2*$^{-/-}$ synapses.

Although in murine neurons interference with GIT1 function changes dendrite morphogenesis and morphology (Zhang et al., 2003), it remains unknown if GIT proteins affect presynaptic morphology. Despite C_{slow} values indicate that loss of GITs did not affect calyx size (Figure 3K), C_{slow} values do not report the actual calyx size, but the capacitance of the calyx and the variable length of axon that remains attached (Borst and Sakmann, 1998). Therefore, to accurately quantitate if calyx morphology was altered by the loss of GITs, we carried out 3D reconstructions from confocal z-stack images of WT, *Git2*$^{-/-}$, *Git1*$^{-/-}$, or *Git1*$^{-/-}$/*Git2*$^{-/-}$ calyces and determined the surface area and volume from the P18-21 calyces (Figure 4E–I). Analysis revealed no surface area reduction in the *Git2*$^{-/-}$, *Git1*$^{-/-}$, or *Git1*$^{-/-}$/*Git2*$^{-/-}$ calyces compared to WT (Figure 4F, G, table S1). However, despite no change in surface area, there was an increase in the volume of *Git2*$^{-/-}$ calyces

compared to WT (880.50 ± 59.17 μm^3, n=29 vs. 639.60 ± 41.46 μm^3, n=29; $p < 0.05$) (Figure 4H, I, table S1). Nevertheless, based on the absence of surface area and volume changes in *Git1*$^{-/-}$ or *Git1*$^{-/-}$/*Git2*$^{-/-}$, we conclude that the increased exocytosis efficiency due to increases of P_r, with loss of GIT1, and further synaptic strength increase in the absence of GIT1 and GIT2 are not due to altered calyx morphology.

Discussion

In our present study, we tested whether GIT proteins have a role in presynaptic regulation of mammalian synaptic function. Using our ability to selectively study GITs presynaptic function, we conclude that GIT1 and GIT2 proteins regulate synaptic strength by increasing the exocytosis efficiency through distinct mechanisms: GIT1 by negatively regulating P_r, while GIT2 acts through an unknown mechanism.

Although GIT1 and GIT2 share the same domain structure, they appear to have some distinct functions at the molecular level (Hoefen and Berk, 2006) and behaviorally (Schmalzigaug et al., 2009a; Schmalzigaug et al., 2009b). Only loss of GIT1 alone led to an increase in P_r while no further increases in P_r were seen with loss of both GIT1 and GIT2. These GIT isoform differences of P_r regulation might be explained by high levels of GIT1 expression relative to GIT2 in the calyx, GIT1 mRNA levels are ~10 fold higher than GIT2 mRNA levels (Korber et al., 2014), or by GIT2 having an independent mechanism for regulating synaptic strength. Nonetheless, it is clear that GIT2 contributes to regulation of presynaptic function as the combined loss of GIT1 and GIT2 is required to significantly increase AP-evoked EPSCs. At the calyx, P_r is reduced during development (Iwasaki and Takahashi, 2001; Taschenberger and von Gersdorff, 2000). Although increases in GIT1 and GIT2 expression levels after hearing onset may contribute to P_r reduction, GIT mRNA levels in GBCs are unchanged before and after hearing (Korber et al., 2014).

The RRP consists of two SVs populations, those which are readily releasable and those which are reluctant to be released in response to an AP. The regulation of the number that are readily releasable directly effects initial P_r (Neher, 2010). CAZ proteins have emerged as potential regulators of P_r through different mechanisms: 1) Positional priming, which regulates SV to VGCC coupling (Neher, 2010). 2) Post priming, which regulates downstream signaling cascades after positional priming that lower the energy barrier for fusion (Lee et al., 2013). At the calyx, positional priming is tightly regulated to ensure continuous SV availability for encoding auditory information (Chen et al., 2015; Fedchyshyn and Wang, 2005; Nakamura et al., 2015). However, understanding of the molecular mechanisms that regulate positional priming is still in the early stages. At the calyx, Munc13-1 has been suggested to positively regulate positional priming by bringing SVs closer to the VGCCs (Chen et al., 2013). At hippocampal synapses the actin cytoskeleton is implied to be a structural barrier which prevents close association between SVs and VGCCs, thereby serving as negative regulators of positional priming (Cingolani and Goda, 2008). Studies at the calyx on Septin 5 (Yang et al., 2010) and those that acutely disrupt the actin cytoskeleton (Lee et al., 2012) demonstrate that these structural barriers can serve as negative regulators of SV release in response to an AP and affect P_r. Since GIT1 is located at the AZ at the same distance as RIM proteins with respect to Bassoon (Podufall et

al., 2014), it is possible that GIT/PIX complexes might regulate actin dynamics at the AZ which affects positional priming of SVs. Evidence supporting this hypothesis comes from a study in which knockdown of Piccolo, a regulator of F-actin dynamics and a GIT binding protein, results in facilitation of SV exocytosis and increases the rates of depression (Waites et al., 2011). Future studies will be needed to address this possibility.

Our data cannot rule out a possible role for GITs in post priming. Previous studies revealed that modulation of lipid signaling at the AZ can change P_r (Basu et al., 2007; Lee et al., 2013). GITs deactivate Arf6 which in turn can regulate the production of lipids PA and PIP_2 (Hoefen and Berk, 2006). Work in neuroendocrine cells suggests that GITs negatively regulate Arf6 pathways to inhibit exocytosis (Meyer et al., 2006). However, the granule docking site in neuroendocrine cells is different from the AZ in neurons and have different release rates. Thus, the mechanisms of GIT function found in neuroendocrine cells will need to be verified in neurons.

Our findings on the functional role of GIT proteins at the calyx define a different phenotype than reported in a *Drosophila* transgenic model where dGIT function was analyzed at the NMJ (Podufall et al., 2014). These differences might be due to: 1) sequence differences between the mammalian GIT and *Drosophila* dGITproteins (43% similar) (Bahri et al., 2009); 2) complete deletion of GIT proteins in our study, and hypomorphs in *Drosophila*; 3) differences in AZ organization at the fly NMJ compared to a mammalian AZ (Zhai and Bellen, 2004). Differing results with GITs across species is not unreasonable, as disruption of the ELKS/CAST homolog *bruchpilot* (Kaeser et al., 2009) differentially effects synaptic transmission in *Drosophila* and mammals. Interestingly, disruption of dGIT function in high external Ca^{2+} did lead to increased presence of synaptopHluorin on the plasma membrane at 10 and 50 Hz. This result could be interpreted as the loss of GIT results in an increase in P_r at the *Drosophila* NMJ, which would be consistent with our findings in the calyx. Finally, dGIT regulates endocytosis in *Drosophila*, but it remains to be tested in mammals.

In summary, we have demonstrated for the first time that GITs are important presynaptic regulators of synaptic strength. This regulation of synaptic strength by GITs is likely to contribute to the disruption of the neuronal circuit output that leads to hearing loss phenotypes, impairment in fear memory, and spatial and object learning. Future studies will resolve the mechanisms by which GITs regulate RRP dynamics and their roles in the early stages of auditory processing and neurological diseases.

EXPERIMENTAL PROCEDURES

Detailed methods are in Supplemental Experimental Procedures.

Afferent fiber stimulation and presynaptic recordings were performed as previously described on P16-21 mice (Chen et al., 2013; Chen et al., 2015). Confocal images were acquired with a Zeiss LSM 780 and analysed using Amira 5.6 and Fiji imaging analysis software. For EM experiments, Tecnai G2 Spirit BioTwin TEM was used and images were taken with a Veleta CCD camera (Olympus) operated by TIA software (FEI) and analyzed

using Fiji. All procedures were performed in accordance with the animal welfare guidelines of MPFI Institutional Animal Care and Use Committee.

Supplementary Material

Refer to Web version on PubMed Central for supplementary material.

Acknowledgments

We thank Dr. Holger Taschenberger for sharing custom mEPSC analysis routine. We thank Drs. Lu-Yang Wang, Brock Grill and Kirill Martemyanov for comments on the manuscript. This work was supported by the Max Planck Society and a NIH R01 grant from the National Institute on Deafness and Other Communication Disorders DC014093-01 awarded to S.M.Y., Jr. and NIH R21 MH090556 and DoD W81XWH-11-2-0112 awarded to R.T.P.

References

1. Bahri SM, Choy JM, Manser E, Lim L, Yang X. The Drosophila homologue of Arf-GAP GIT1, dGIT, is required for proper muscle morphogenesis and guidance during embryogenesis. Developmental biology. 2009; 325:15–23. [PubMed: 18996366]
2. Basu J, Betz A, Brose N, Rosenmund C. Munc13-1 C1 domain activation lowers the energy barrier for synaptic vesicle fusion. The Journal of neuroscience. 2007; 27:1200–1210. [PubMed: 17267576]
3. Borst JG, Sakmann B. Calcium current during a single action potential in a large presynaptic terminal of the rat brainstem. The Journal of physiology. 1998; 506(Pt 1):143–157. [PubMed: 9481678]
4. Borst JG, Soria van Hoeve J. The calyx of held synapse: from model synapse to auditory relay. Annual review of physiology. 2012; 74:199–224.
5. Chen Z, Cooper B, Kalla S, Varoqueaux F, Young SM Jr. The Munc13 proteins differentially regulate readily releasable pool dynamics and calcium-dependent recovery at a central synapse. The Journal of neuroscience : the official journal of the Society for Neuroscie. 2013; 33:8336–8351.
6. Chen Z, Das B, Nakamura Y, DiGregorio DA, Young SM Jr. Ca2+ channel to synaptic vesicle distance accounts for the readily releasable pool kinetics at a functionally mature auditory synapse. The Journal of neuroscience. 2015; 35:2083–2100. [PubMed: 25653365]
7. Cingolani LA, Goda Y. Actin in action: the interplay between the actin cytoskeleton and synaptic efficacy. Nature reviews Neuroscience. 2008; 9:344–356. [PubMed: 18425089]
8. Elmqvist D, Quastel DM. A quantitative study of end-plate potentials in isolated human muscle. The Journal of physiology. 1965; 178:505–529. [PubMed: 5827910]
9. Fedchyshyn MJ, Wang LY. Developmental transformation of the release modality at the calyx of Held synapse. The Journal of neuroscience. 2005; 25:4131–4140. [PubMed: 15843616]
10. Goehler H, Lalowski M, Stelzl U, Waelter S, Stroedicke M, Worm U, Droege A, Lindenberg KS, Knoblich M, Haenig C, et al. A protein interaction network links GIT1, an enhancer of huntingtin aggregation, to Huntington's disease. Molecular cell. 2004; 15:853–865. [PubMed: 15383276]
11. Gundelfinger ED, Fejtova A. Molecular organization and plasticity of the cytomatrix at the active zone. Current opinion in neurobiology. 2012; 22:423–430. [PubMed: 22030346]
12. Hoefen RJ, Berk BC. The multifunctional GIT family of proteins. Journal of cell science. 2006; 119:1469–1475. [PubMed: 16598076]
13. Iwasaki S, Takahashi T. Developmental regulation of transmitter release at the calyx of Held in rat auditory brainstem. The Journal of physiology. 2001; 534:861–871. [PubMed: 11483715]
14. Kaeser PS, Deng L, Chavez AE, Liu X, Castillo PE, Sudhof TC. ELKS2alpha/CAST deletion selectively increases neurotransmitter release at inhibitory synapses. Neuron. 2009; 64:227–239. [PubMed: 19874790]
15. Kim S, Ko J, Shin H, Lee JR, Lim C, Han JH, Altrock WD, Garner CC, Gundelfinger ED, Premont RT, et al. The GIT family of proteins forms multimers and associates with the presynaptic

cytomatrix protein Piccolo. The Journal of biological chemistry. 2003; 278:6291–6300. [PubMed: 12473661]

16. Klein M, van der Voet M, Harich B, van Hulzen KJ, Onnink AM, Hoogman M, Guadalupe T, Zwiers M, Groothuismink JM, Verberkt A, et al. Converging evidence does not support GIT1 as an ADHD risk gene. American journal of medical genetics Part B, Neuropsychiatric genetics : the official publication of the International Society of Psychiatric Genetics. 2015
17. Ko J, Kim S, Valtschanoff JG, Shin H, Lee JR, Sheng M, Premont RT, Weinberg RJ, Kim E. Interaction between liprin-alpha and GIT1 is required for AMPA receptor targeting. The Journal of neuroscience. 2003; 23:1667–1677. [PubMed: 12629171]
18. Korber C, Dondzillo A, Eisenhardt G, Herrmannsdorfer F, Wafzig O, Kuner T. Gene expression profile during functional maturation of a central mammalian synapse. The European journal of neuroscience. 2014; 40:2867–2877. [PubMed: 24995587]
19. Lee JS, Ho WK, Lee SH. Actin-dependent rapid recruitment of reluctant synaptic vesicles into a fast-releasing vesicle pool. Proceedings of the National Academy of Sciences of the United States of America. 2012; 109:E765–E774. [PubMed: 22393020]
20. Lee JS, Ho WK, Neher E, Lee SH. Superpriming of synaptic vesicles after their recruitment to the readily releasable pool. Proceedings of the National Academy of Sciences of the United States of America. 2013; 110:15079–15084. [PubMed: 23980146]
21. Lucanic M, Cheng HJ. A RAC/CDC-42-independent GIT/PIX/PAK signaling pathway mediates cell migration in C. elegans. PLoS genetics. 2008; 4:e1000269. [PubMed: 19023419]
22. Menon P, Deane R, Sagare A, Lane SM, Zarcone TJ, O'Dell MR, Yan C, Zlokovic BV, Berk BC. Impaired spine formation and learning in GPCR kinase 2 interacting protein-1 (GIT1) knockout mice. Brain research. 2010; 1317:218–226. [PubMed: 20043896]
23. Meyer MZ, Deliot N, Chasserot-Golaz S, Premont RT, Bader MF, Vitale N. Regulation of neuroendocrine exocytosis by the ARF6 GTPase-activating protein GIT1. The Journal of biological chemistry. 2006; 281:7919–7926. [PubMed: 16439353]
24. Nakamura Y, Harada H, Kamasawa N, Matsui K, Rothman JS, Shigemoto R, Silver RA, DiGregorio DA, Takahashi T. Nanoscale distribution of presynaptic Ca(2+) channels and its impact on vesicular release during development. Neuron. 2015; 85:145–158. [PubMed: 25533484]
25. Neher E. What is Rate-Limiting during Sustained Synaptic Activity: Vesicle Supply or the Availability of Release Sites. Frontiers in synaptic neuroscience. 2010; 2:144. [PubMed: 21423530]
26. Podufall J, Tian R, Knoche E, Puchkov D, Walter AM, Rosa S, Quentin C, Vukoja A, Jung N, Lampe A, et al. A presynaptic role for the cytomatrix protein GIT in synaptic vesicle recycling. Cell reports. 2014; 7:1417–1425. [PubMed: 24882013]
27. Regehr WG. Short-term presynaptic plasticity. Cold Spring Harbor perspectives in biology. 2012; 4:a005702. [PubMed: 22751149]
28. Schikorski T, Stevens CF. Morphological correlates of functionally defined synaptic vesicle populations. Nature neuroscience. 2001; 4:391–395. [PubMed: 11276229]
29. Schmalzigaug R, Phee H, Davidson CE, Weiss A, Premont RT. Differential expression of the ARF GAP genes GIT1 and GIT2 in mouse tissues. The journal of histochemistry and cytochemistry : official journal of the Histochemistry Society. 2007; 55:1039–1048. [PubMed: 17565117]
30. Schmalzigaug R, Rodriguiz RM, Bonner PE, Davidson CE, Wetsel WC, Premont RT. Impaired fear response in mice lacking GIT1. Neuroscience letters. 2009a; 458:79–83. [PubMed: 19383529]
31. Schmalzigaug R, Rodriguiz RM, Phillips LE, Davidson CE, Wetsel WC, Premont RT. Anxiety-like behaviors in mice lacking GIT2. Neuroscience letters. 2009b; 451:156–161. [PubMed: 19114090]
32. Schneggenburger R, Meyer AC, Neher E. Released fraction and total size of a pool of immediately available transmitter quanta at a calyx synapse. Neuron. 1999; 23:399–409. [PubMed: 10399944]
33. Segura I, Essmann CL, Weinges S, Acker-Palmer A. Grb4 and GIT1 transduce ephrinB reverse signals modulating spine morphogenesis and synapse formation. Nature neuroscience. 2007; 10:301–310. [PubMed: 17310244]

34. Taschenberger H, Leao RM, Rowland KC, Spirou GA, von Gersdorff H. Optimizing synaptic architecture and efficiency for high-frequency transmission. Neuron. 2002; 36:1127–1143. [PubMed: 12495627]

35. Taschenberger H, von Gersdorff H. Fine-tuning an auditory synapse for speed and fidelity: developmental changes in presynaptic waveform, EPSC kinetics, and synaptic plasticity. The Journal of neuroscience. 2000; 20:9162–9173. [PubMed: 11124994]

36. Waites CL, Leal-Ortiz SA, Andlauer TF, Sigrist SJ, Garner CC. Piccolo regulates the dynamic assembly of presynaptic F-actin. The Journal of neuroscience. 2011; 31:14250–14263. [PubMed: 21976510]

37. White JK, Gerdin AK, Karp NA, Ryder E, Buljan M, Bussell JN, Salisbury J, Clare S, Ingham NJ, Podrini C, et al. Genome-wide generation and systematic phenotyping of knockout mice reveals new roles for many genes. Cell. 2013; 154:452–464. [PubMed: 23870131]

38. Won H, Mah W, Kim E, Kim JW, Hahm EK, Kim MH, Cho S, Kim J, Jang H, Cho SC, et al. GIT1 is associated with ADHD in humans and ADHD-like behaviors in mice. Nature medicine. 2011; 17:566–572.

39. Yang YM, Fedchyshyn MJ, Grande G, Aitoubah J, Tsang CW, Xie H, Ackerley CA, Trimble WS, Wang LY. Septins regulate developmental switching from microdomain to nanodomain coupling of Ca(2+) influx to neurotransmitter release at a central synapse. Neuron. 2010; 67:100–115. [PubMed: 20624595]

40. Yang YM, Wang LY. Amplitude and kinetics of action potential-evoked Ca2+ current and its efficacy in triggering transmitter release at the developing calyx of held synapse. The Journal of neuroscience. 2006; 26:5698–5708. [PubMed: 16723526]

41. Zhai RG, Bellen HJ. The architecture of the active zone in the presynaptic nerve terminal. Physiology (Bethesda). 2004; 19:262–270. [PubMed: 15381754]

42. Zhang H, Webb DJ, Asmussen H, Horwitz AF. Synapse formation is regulated by the signaling adaptor GIT1. The Journal of cell biology. 2003; 161:131–142. [PubMed: 12695502]

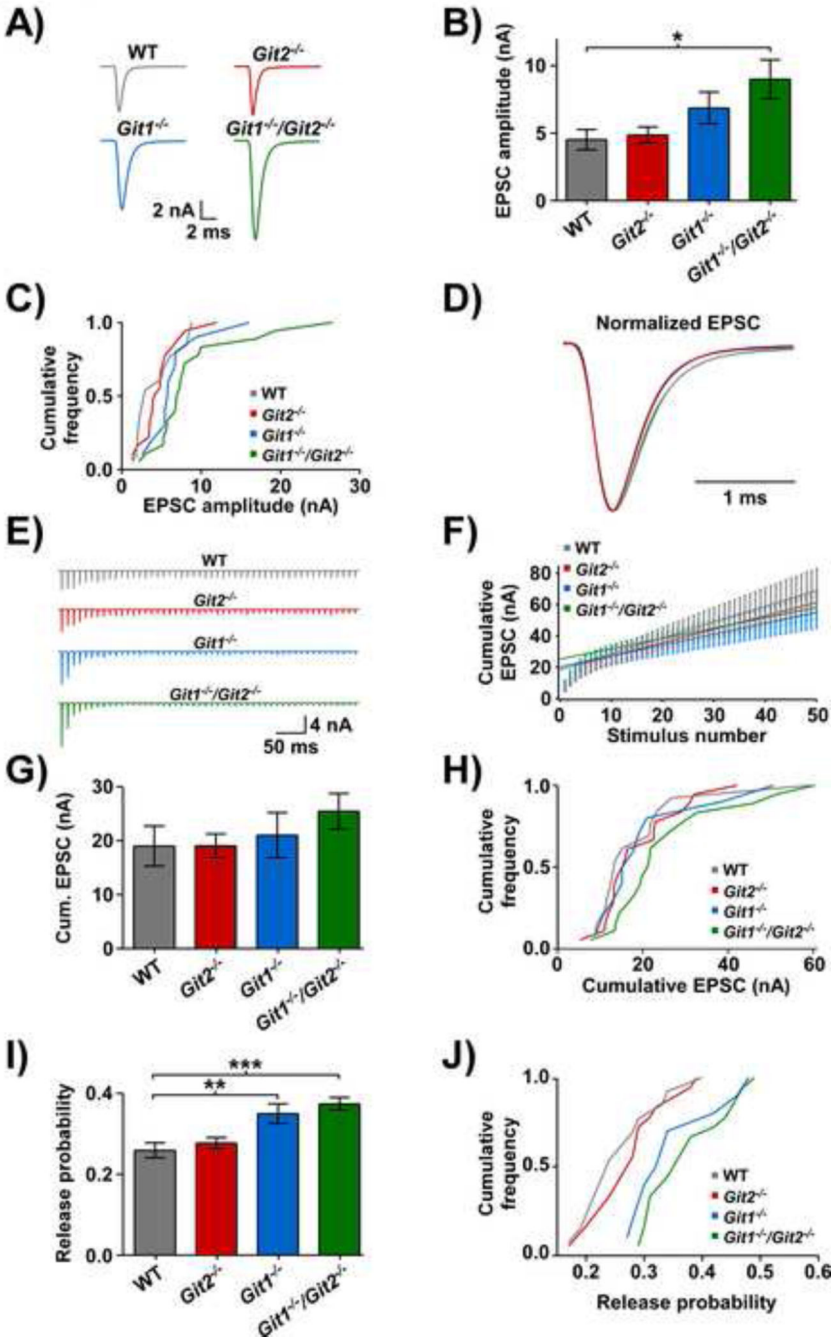

Figure 1. GIT proteins regulate AP-evoked release and P_r

A) Representative traces of single AP-evoked EPSCS from WT, *Git2*$^{-/-}$, *Git1*$^{-/-}$, or *Git1*$^{-/-}$/*Git2*$^{-/-}$ calyces. **B)** Summary data showing average EPSC amplitudes. **C)** Cumulative frequency histogram of EPSC amplitudes. **D)** Average normalized EPSC amplitudes. **E)** Example traces in response to a 100Hz stimulus train from WT, *Git2*$^{-/-}$, *Git1*$^{-/-}$, or *Git1*$^{-/-}$/*Git2*$^{-/-}$ calyces. **F)** Cumulative plots of EPSC amplitudes with back-extrapolated linear fits. **G)** Average values for the calculated RRP size. **H)** Cumulative frequency histogram of RRP size. **I)** P_r obtained by dividing the amplitude of the first EPSC from the 100Hz train by the

calculated RRP size. **J)** Cumulative frequency histogram of P_r. *p<0.05, **p<0.01, ***p<0.001 One-way ANOVA with a *post hoc* Dunnett's test.

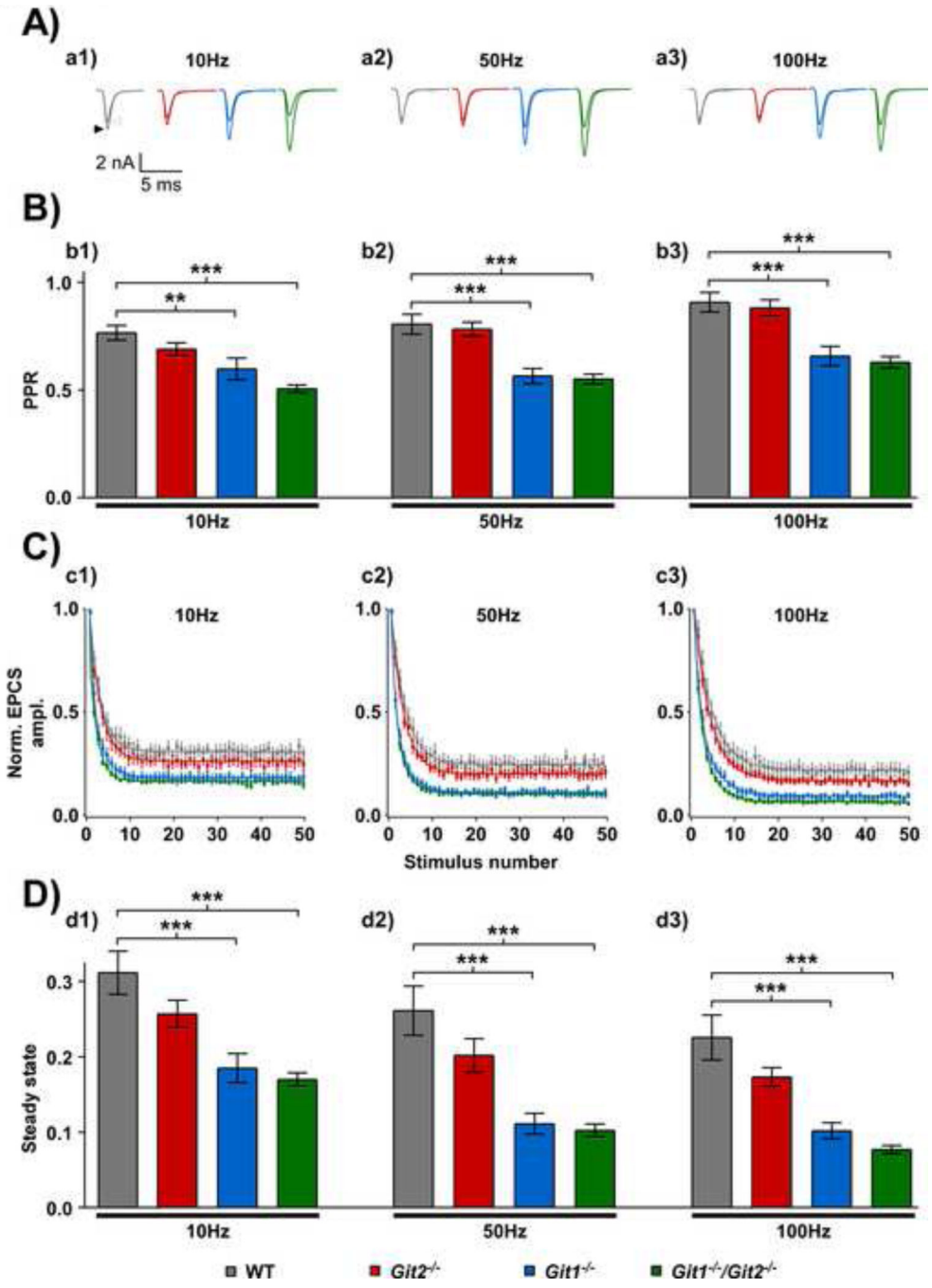

Figure 2. Synaptic plasticity is altered by the loss of GIT expression

A) Example traces of the EPSC obtained by fiber stimulation after applying two consecutive pulses at the frequencies indicated (**a1**, 10Hz; **a2**, 50Hz; **a3**, 100Hz). Black and white arrow heads indicate the 1st and 2nd EPSC, respectively. **B)** PPR was calculated by dividing the amplitude of the second EPSC by the amplitude of the first EPSC at 10Hz (**b1**), 50Hz (**b2**) and 100Hz (**b3**). **C)** Summary plot of normalized EPSC amplitude to the first EPSC during train stimuli using 10Hz **(c1)**, 50Hz **(c2)** and 100Hz **(c3)** against the stimulus number. **D)** Steady state depression level measured and plotted as a function of the stimulation

frequency (**d1**, 10Hz; **d2**, 50Hz; **d3**, 100Hz). **p<0.01, ***p<0.001 One-way ANOVA with a *post hoc* Dunnett's test.

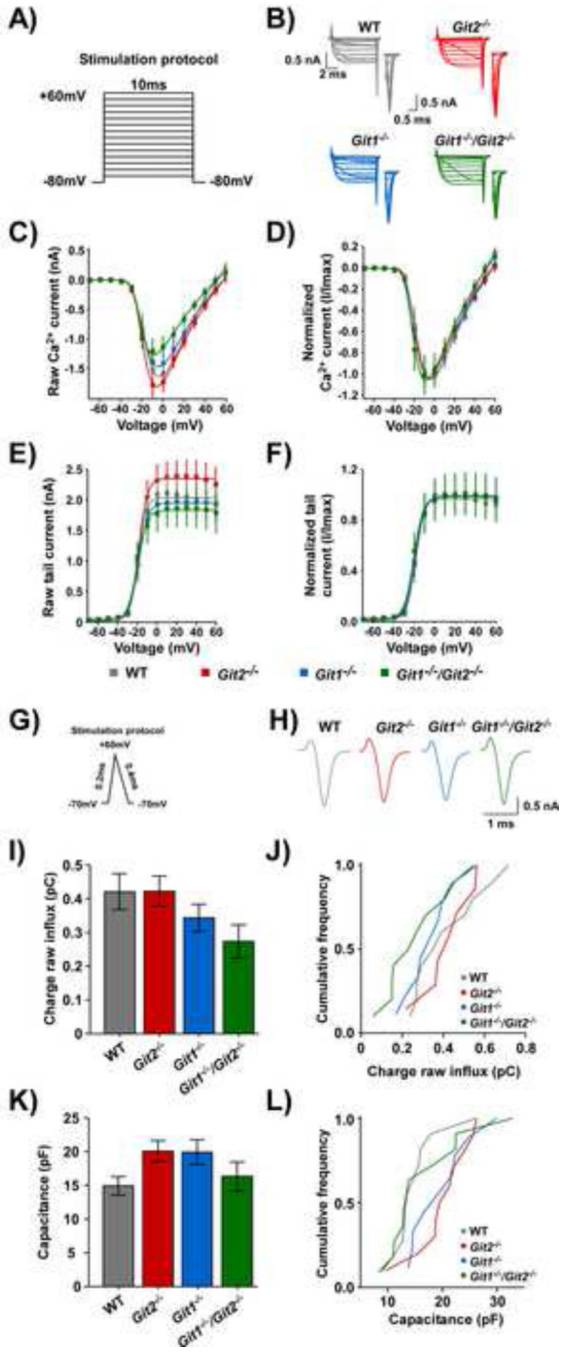

Figure 3. Loss of GIT proteins results in no changes of Ca^{2+} current and activation kinetics

A) Stimulus protocol used for the experiment from B to F. **B)** Representative I_{Ca} traces for I/V curve analysis from −80mV to +60mV from WT, *Git2*$^{-/-}$, *Git1*$^{-/-}$ and *Git1*$^{-/-}$/*Git2*$^{-/-}$ calyces. Insets show in detail the tail currents. **C)** I/V plot representing the average steady state I_{Ca} amplitudes plotted against voltage. **D)** Normalized average raw I_{Ca} amplitudes to Imax. **E)** Analysis of voltage dependent activation of VGCCs. **F)** Normalized tail currents to Imax. **G)** Stimulus protocol used for the experiment from H to L. **H)** Representative I_{Ca} obtained from WT, *Git2*$^{-/-}$, *Git1*$^{-/-}$ and *Git1*$^{-/-}$/*Git2*$^{-/-}$ calyces. **I)** Average values of I_{Ca}

charge. **J)** Cumulative frequency of I_{Ca} charge. **K**) Average values of capacitance (C_{slow}). **L)** Cumlative frequency of C_{slow}.

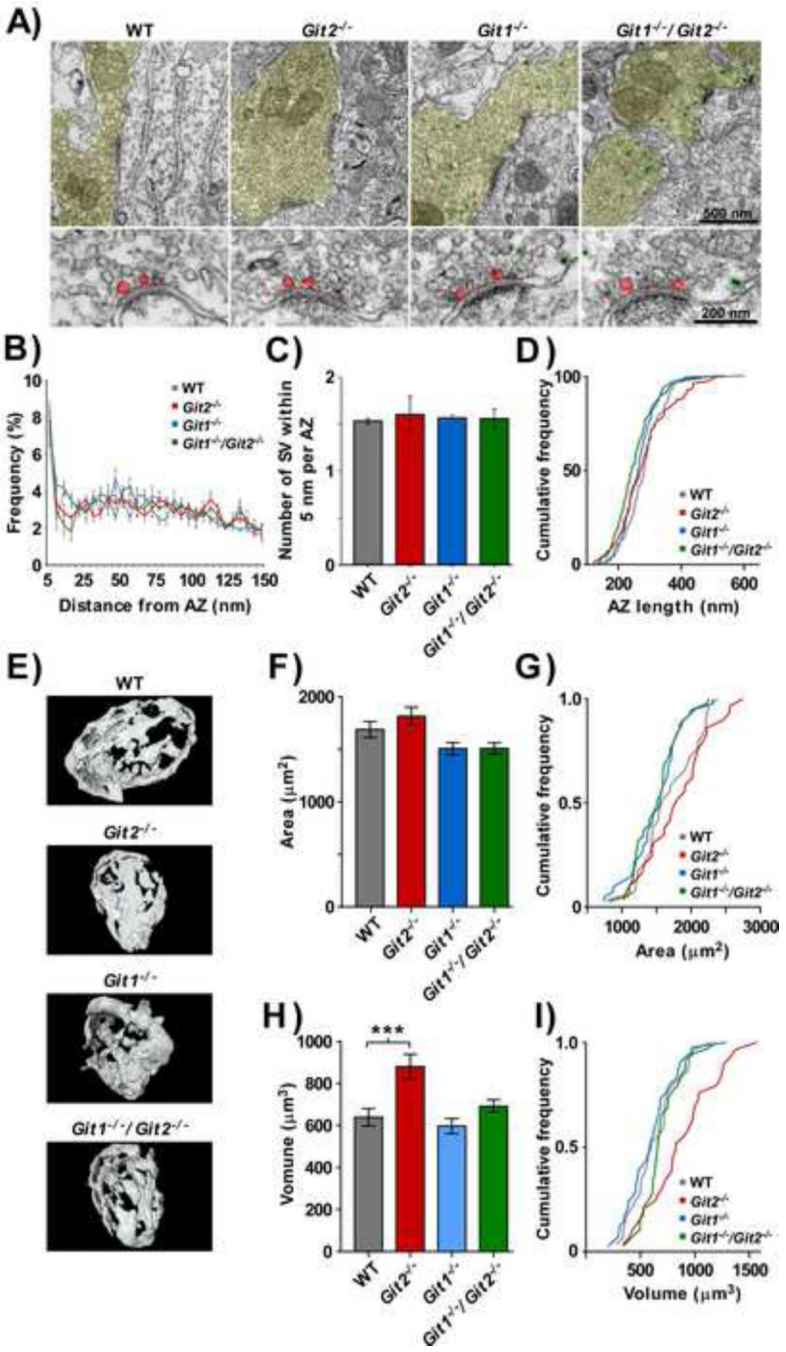

Figure 4. Ablation of GIT expression does not affect the number of docked SV or SV distribution

A) EM sample images taken from WT, *Git2*$^{-/-}$, *Git1*$^{-/-}$ and *Git1*$^{-/-}$/*Git2*$^{-/-}$ calyces. Top panels: calyx of Held is demarcated in yellow, and the nanogold GFP labeling in green (scale bar=500 nm). Bottom panels: detail of the AZ analyzed. SVs closest to the AZ are shown in red shade and AZ length is been denoted by a red line (scale bar=200 nm). **B)** Summary of normalized distribution of SV distance from AZs. **C)** Average number of SVs localized within 5 nm relative to the AZs. **D)** Cumulative frequency histogram of the AZ length. **E)** Example of 3D reconstructions from WT, *Git2*$^{-/-}$, *Git1*$^{-/-}$ and *Git1*$^{-/-}$/*Git2*$^{-/-}$

calyces. **F)** Average values of surface area and the corresponding cumulative frequency distribution in G). **H)** Summary data showing average values of volume and the corresponding cumulative frequency distribution in I).